Materials Research Bulletin 143 (2021) 111460

Contents lists available at ScienceDirect

Materials Research Bulletin

journal homepage: www.elsevier.com/locate/matresbu

Research Papers

Surface properties enhancement by sulfur-doping TiO_2 films

Rodrigo Teixeira Bento [a], Olandir Vercino Correa [a], Renato Altobelli Antunes [b], Marina Fuser Pillis [a,*]

[a] Nuclear and Energy Research Institute, IPEN/CNEN, Brazil
[b] Federal University of ABC, UFABC, Brazil

ARTICLE INFO

Keywords:
Titanium dioxide
MOCVD
Sulfur-doped TiO_2
Surface modification
Photocatalysis

ABSTRACT

TiO_2 films were sulfur-doped through an alternative route based on the decomposition of H_2S at low temperatures. MOCVD technique was used to grown the films on borosilicate glass substrates at 400 °C. The doping was carried out at 50, 100 and 150 °C under a mixture of H_2-2%v.H_2S. SO_4^{2-} groups were observed in the surface revealing the substitution of Ti^{4+} by S^{6+}. Superficial roughness and wettability were also modified by the formation of these sulfate groups on the surface. Photocatalytic experiments of methyl-orange dye decolorization under visible light indicated that the 8 at.% S-TiO_2 film exhibited the highest photocatalytic activity, with 72.1% of dye decolorization. The results suggest that the exposition of TiO_2 films to the mixture H_2-H_2S at low temperatures is an efficient method of doping. These films allow the decolorization of the dye under visible light irradiation, which enable its practical use under sunlight or even indoor.

1. Introduction

Titanium dioxide (TiO_2) films have been extensively employed on materials Engineering due to the good performance demonstrated against corrosion, the self-cleaning characteristics, the relatively low cost of production, and the excellent photocatalytic behavior [1–8]. Metalorganic chemical vapor deposition (MOCVD) is a widely used technique to synthesize TiO_2 films. In this method, the chemical constituents react on the surface of the heated substrate, forming a solid, continuous and adherent film [9]. This method offers good control of stoichiometry and thickness of the films, uniformity of deposition, and allows the covering of large areas [10,11].

In the recent years, several papers demonstrate the potential use of metals and/or non-metals elements, such as transition metals (Co, Ni, and Cu), rare earth, C, N, and S, for doping and surface modification of TiO_2 films – often reported as one of the most effective methods of increasing its efficiency on environmental applications [8,12–14]. Toxic gases associated to atmospheric pollution, such as ammonia (NH_3), fluorine (F_2), chlorine (Cl_2), bromine (Br_2), and hydrogen sulfide (H_2S) have also been used in TiO_2 doping process [15–17]. Studies aimed to the use of H_2S exhibited good results [18–21]. The H_2S decomposition and sulfur adsorption on the TiO_2 surface process can be conducted under atmospheric pressure, at low temperatures [22,23], and occurs due to the presence of hydroxyl radicals ($^{\bullet}OH$) on the films surface, which favors sulfur oxidation [24]. Consequently, SO_4^{2-} sulphate groups are formed on the TiO_2 surface [2,25]. However, the scientific community until then had not observed that this effect promotes the surface modification and sulfur-doping of the TiO_2 and allows its promising use on water treatment by a green method.

In our previous study [26], 280 nm thick TiO_2 films were sulfur-doped at 50 °C from a H_2-2v.% H_2S gaseous mixture. That research evaluated the behavior of thinner films, and the influence of the luminous intensity on its photoactivity. Nevertheless, the effects of the surface modification of sulfur-doped TiO_2 films obtained by the H_2S decomposition at low temperature remains little investigated. Furthermore, TiO_2 films are usually doped during the growth process [14,15]. Thus, further research is necessary toward the practical application of this innovative method.

In this paper, 470 nm thick TiO_2 films were doped by a low-temperature alternative route, and then characterized. The films were grown by MOCVD and posteriorly sulfur-doped at three different temperatures 50, 100 and 150 °C in H_2/H_2S atmosphere in order to allow different concentrations of sulfur to be incorporated into the films. The effect of sulfur-doping by a process similar to that used for the H_2S desulfurization on the structure properties, morphological characteristics, and dye decolorization behavior of the films were also studied.

* Corresponding author.
E-mail address: mfpillis@ipen.br (M.F. Pillis).

https://doi.org/10.1016/j.materresbull.2021.111460
Received 5 March 2021; Received in revised form 21 June 2021; Accepted 23 June 2021
Available online 1 July 2021

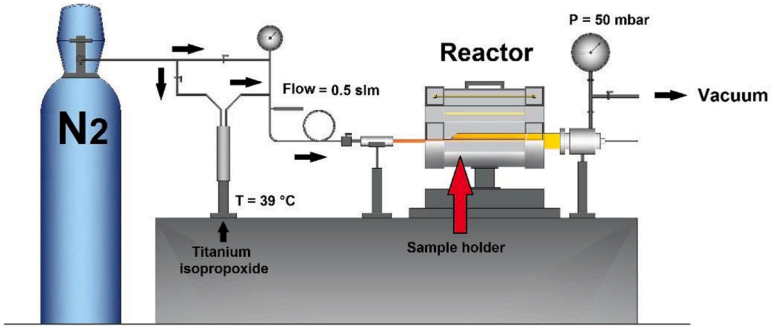

Fig. 1. Illustrative scheme of the MOCVD equipment used for the growth of TiO_2 films.

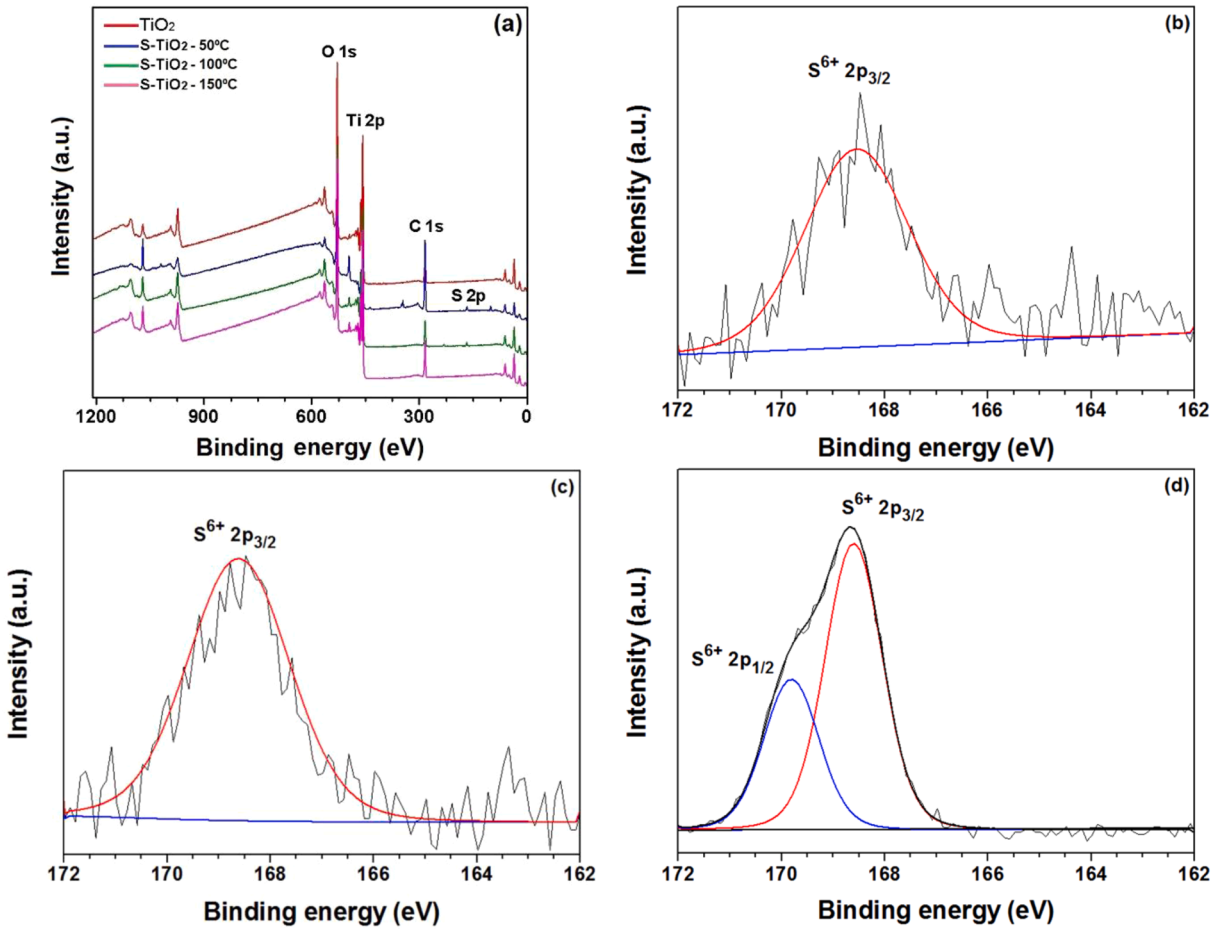

Fig. 2. (a) XPS survey spectra of the undoped and sulfur-doped at 50 °C, 100 °C and 150 °C TiO_2 films; high-resolution XPS spectrum of the S 2p region with the fitted curves for (b) 0.2 at.% S into TiO_2 film; (c) 3 at.% S into TiO_2 film; (d) 8 at.% S into TiO_2 film.

Table 1
Elemental analyses of undoped and sulfur-doped TiO_2 films.

	Ti (at%)	O (at%)	C (at%)	S (at%)
Undoped TiO_2	28.2	62.5	9.3	-
S-TiO_2 – 50 °C	21.6	52.4	17.9	8.1
S-TiO_2 – 100 °C	24.5	59.8	12.6	3.1
S-TiO_2 – 150 °C	25.9	59.4	14.5	0.2

2. Experimental

2.1. Growth of TiO_2 films

The 470 nm-thick TiO_2 films were grown by MOCVD process in a conventional horizontal homemade reactor earlier described by Bento and Pillis [3]. Previous studies showed the existence of an adequate thickness – around 400 nm – in which the films present the best behavior [27]. Borosilicate glass was used as substrate (25 × 76 × 1 mm) in view of its low cost. Before the growth the substrates were washed in a 5 % H_2SO_4 aqueous solution, rinsed in deionized water, dried in nitrogen (N_2), and inserted into the deposition chamber. The films growth was performed at 400 °C under 50 mbar of pressure. The titanium and

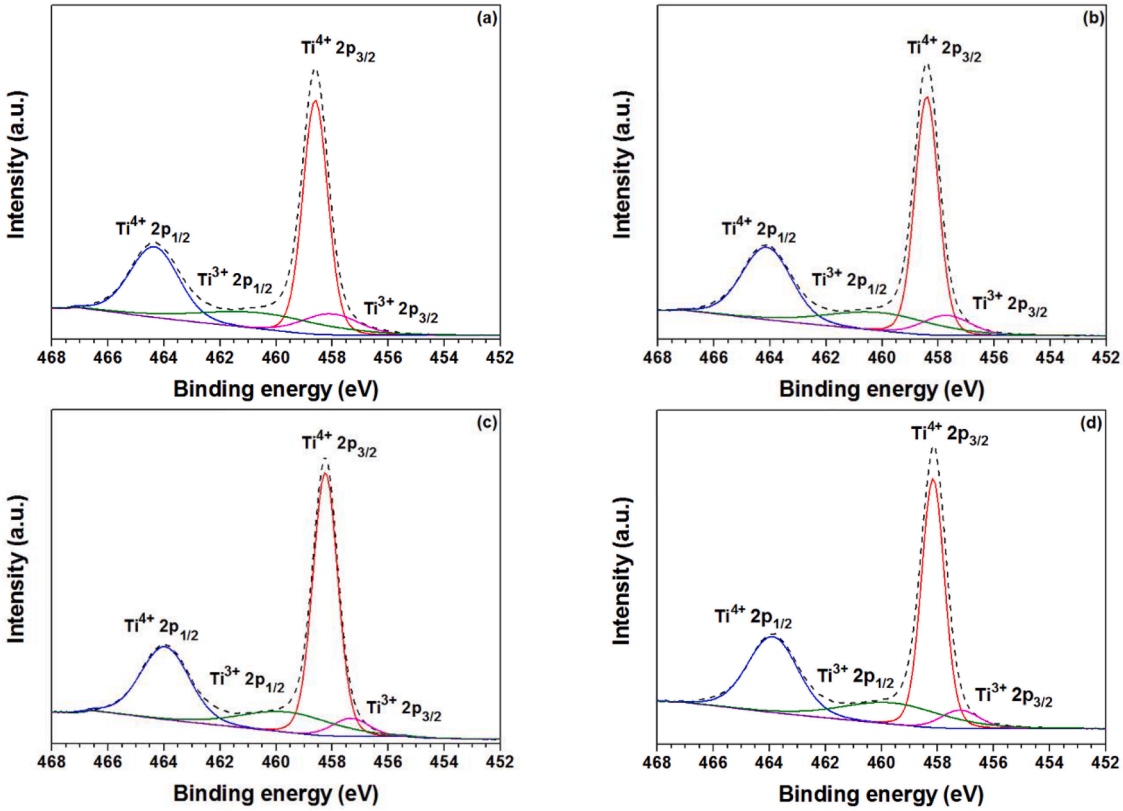

Fig. 3. High-resolution XPS spectra of the Ti 2p region together with the fitted curves: (a) undoped TiO_2 film; (b) 0.2 at.% S into TiO_2 film; (c) 3 at.% S into TiO_2 film; (d) 8 at.% S into TiO_2 film.

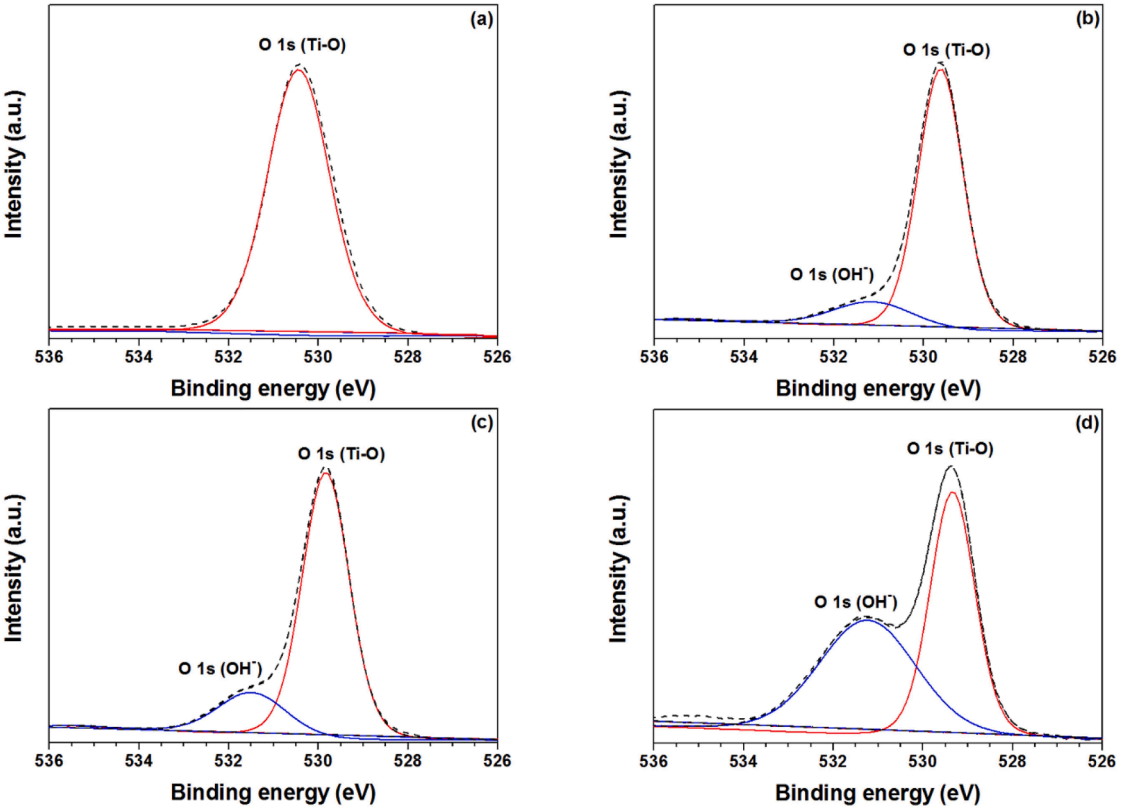

Fig. 4. High-resolution XPS spectra of the O 1s region together with the fitted curves: (a) undoped TiO_2 film; (b) 0.2 at.% S into TiO_2 film; (c), 3 at.% S into TiO_2 film; (d) 8 at.% S into TiO_2 film.

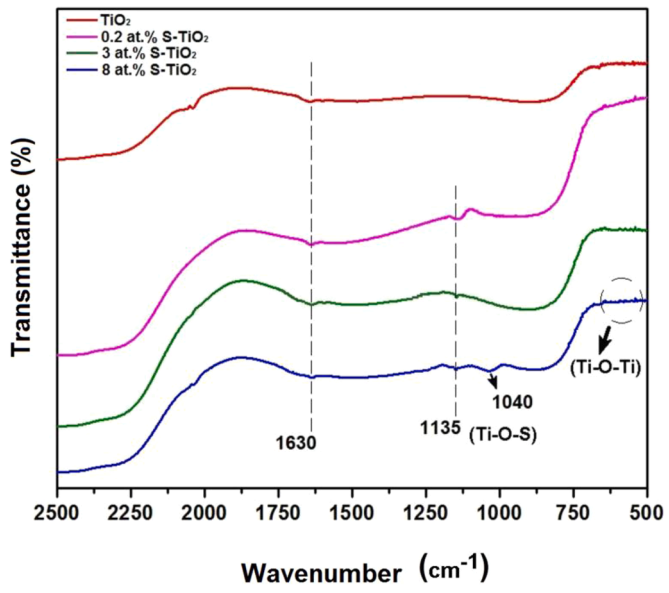

Fig. 5. FTIR spectra of the films of undoped and sulfur-doped TiO_2 films grown by MOCVD at 400 °C.

oxygen sources were Titanium (IV) isopropoxide (TTiP) 99.999 % supplied by *Sigma-Aldrich Co*. Nitrogen was used both as the carrier and purge gases. The flow rates of TTiP and N_2 were fixed at 0.5 slm. Fig. 1 shows schematically the MOCVD equipment.

2.2. Sulfur-doping process

After the TiO_2 films growth, the doping was carried out in a tubular furnace at 50 °C, 100 °C and 150 °C for 60 min under H_2-2v.% H_2S atmosphere, and flow rate set at 0.2 slm. The samples were maintained under argon flux during heating and cooling to room temperature.

2.3. Characterization of the films

X-ray photoelectron spectroscopy (XPS) technique was used to determine the chemical state of the species at the surface. A Thermo Scientific K-Alpha equipment operating with Al-kα radiation source was provided. Survey scans were collected over the 0-1200 eV binding energies range. Higher resolution scans encompassing the principal peaks of Ti 2p, O 1s and S 2p were collected at pass energy of 50 eV. CasaXPS software was used for peak deconvolution [28], and the binding energies were calibrated considering the C1s reference peak at 284.8 eV, attributed to adventitious carbon [14,26]. The Fourier Transform infrared (FTIR) spectra of the films were obtained by using a Thermo Nicolet spectrometer (Nexus 870 FT-IR) in the frequency range of 2500 cm^{-1} to 500 cm^{-1} at room temperature (25 °C). X-ray diffraction (XRD) analyses in the θ-2θ configuration were carried out on a Rigaku Multiflex equipment with a CuKα radiation (λ = 1.54148 Å). The phases formed were identified with the JCPDS (Joint Committee on Powder Diffraction Standards) database. Surface morphology, roughness and mean grain size of the films were determined by atomic force microscopy (AFM) in the tapping mode (SPM Bruker NanoScope IIIA), employing a silicon tip with curvature radius of 15 nm under ambient conditions. Mean grain size were obtained using the ImageJ® image processing software. The wettability of the surface was evaluated by contact angle measurements (SEO Phoenix-i) under visible light. Before the tests, the films were maintained in the dark for 120 h in order to prevent the light interference. The sessile drop method was used by dropping 5 μL of deionized water on the film surface. The experiments were repeated three times for each measurement. The cross-section of the films was evaluated by field emission scanning electron microscopy (FE-SEM) on JSM6701F equipment.

2.4. Photocatalytic tests

The photocatalytic behavior of the films was evaluated by using a homemade reactor setup arranged in a box. The reaction chamber consists of a glass container with 40 mL of the dye solution, the catalysts deposited on borosilicate glass substrate, and the radiation source. Undoped and sulfur-doped TiO_2 films were used as catalysts. An aqueous solution of 0.005 $g.L^{-1}$ of Methyl Orange (MO) dye (pH = 2) was employed as the pollutant model. Several studies suggest that TiO_2 catalysts exhibit better photocatalytic activity under acidic solutions [29–31]. Four tubular LED lamps (Royal Philips Electronics; 3 W; λ = 400~700 nm) were employed as visible light source. The dye decolorization experiments were conducted for a total test time of 300 min. The

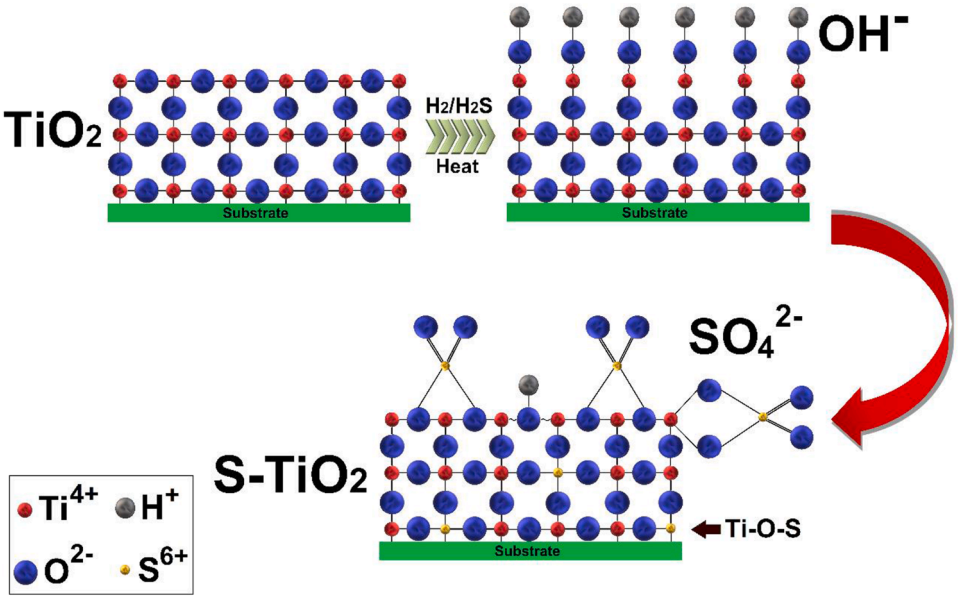

Fig. 6. Scheme demonstrating the proposed coordination models for the bond of SO_4^{2-} sulfate groups and sulfur-doped TiO_2 films.

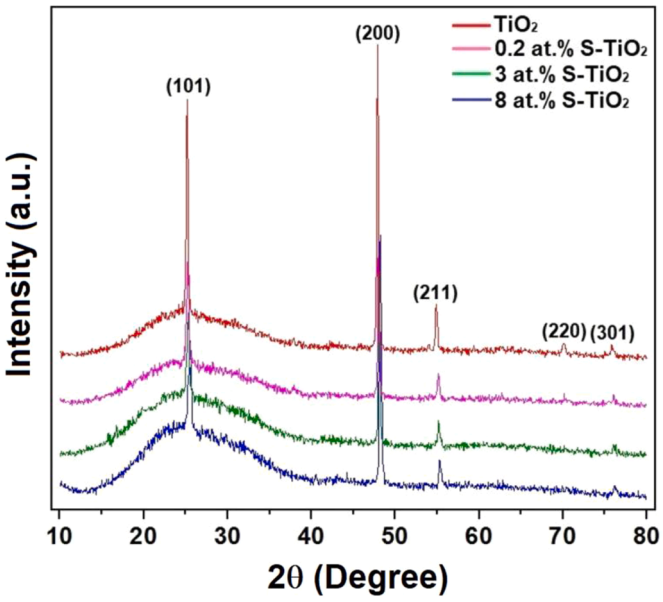

Fig. 7. XRD patterns of the undoped and sulfur-doped TiO_2 films grown on borosilicate glass substrates at 400 °C.

catalyst was disposed 250 mm far from the radiation source. Synthetic air was bubbled into the solution during the tests, in order to homogenize the catalytic reactions, and oxygenate the dye solution. The temperature during experiments was in the range of 19-20 °C. Before the tests the system was kept in the dark under bubbling for one hour for allow the adsorption-desorption equilibrium of the solution on the catalyst surface [27]. The absorbance and pH values of the dye solution were constantly monitored every 30 min. The MO dye concentration changes were examined using a UV-Vis spectrophotometer (Global Trade Technology). After the measurement, the aliquots were returned to the solution.

3. Results and discussion

3.1. Surface chemistry investigation

The comparative XPS survey spectra of the undoped and sulfur-doped TiO_2 films are shown in Fig. 2a. The C 1s peak at 284.8 eV is concerned to the residual carbon from the metalorganic precursor, and to adventitious carbon (C—C or C—H) due to sample exposition to air before the XPS experiments [32,33]. The sulfur-doped TiO_2 survey spectra revealed the presence of a peak of sulfur. The sulfur concentrations of 0.2 at%, 3 at% and 8 at%, are related to films doped at 150 °C, 100 °C and 50 °C, respectively, and is shown in Table 1. The results demonstrated that sulfur concentration in the films decreases as the doping temperature increases. Canela et al. [24] and Bento et al. [26] suggest that the H_2S absorption on the TiO_2 surface is described as dissociative pathways from existing moisture. Since temperature increase promotes evaporation of the water molecules present on the film surface, there is a smaller amount of $^{\bullet}OH$ with which the H_2S molecules can react and oxidize to S ions [22,24].

Fig. 2b-c show the high-resolution XPS spectra of the S 2p region for sulfur-doped TiO_2 films. The S 2p XPS spectrum for 8 at.% S into TiO_2 film (Fig. 2d) showed binding energies at 168.9 eV and 169.8 eV with spin orbit splitting of 0.9 eV. Previous studies indicated that the two energy peaks obtained from the fitted curve could match to S $2p_{3/2}$ and S $2p_{1/2}$, respectively [34–36]. The presence of such energy peaks can be attributed to SO_4^{2-} groups formed on the film surface [23,37]. The 0.2 at % and 3 at.% S into TiO_2 films exhibited only one single peak located at 168.7 eV corresponding to S $2p_{3/2}$. The results indicated the presence of S^{6+} cations, possibly replacing the Ti^{4+} ions [26,38,39], and promoting the formation of Ti-O-S bonds into TiO_2 films [40,41]. The peak at 161 eV was not observed, suggesting that S^{2-}formation does not occur on that surface. Ohno et al. [42] and Umebayashi et al. [43] suggested that it is difficult that O^{2-} can replace S^{2-} due to the differences in the ionic radius (S^{2-} - 0.174 nm, O^{2-} - 0.132 nm).

Fig. 3a-d presents the high resolution XPS spectra of the Ti 2p peak of undoped and sulfur-doped TiO_2 films. It can be seen that there was a minor displacement of the peaks, which may be linked to sulfur doping process [35,36]. Ti 2p region for undoped TiO_2 film (Fig. 3a) presented binding energies at 458.6 eV and 464.3 eV attributed, respectively, to the Ti $2p_{3/2}$ peak [3,44] – which corresponds to Ti^{4+} in TiO_2 lattice [37, 45] – and Ti $2p_{1/2}$ peak [38,42]. Binding energies were identified at 458.4 eV and 464.1 eV for 0.2 at.% S into TiO_2 (Fig. 3b), 458.2 eV and 463.9 eV for 3 at.% S into TiO_2 (Fig. 3c), 458.1 eV and 463.7 eV for 8 at. % S into TiO_2 (Fig. 3d). The doublet peak-to-peak separation (Ti $2p_{3/2}$-Ti $2p_{1/2}$) is 5.6 eV, approximately, according with reported results for anatase-TiO_2 [46]. Anitha et al. [35] and Devi and Kavitha [36] obtained similar results. The authors attributed such behavior to defects formed into the TiO_2 structure by the replacement of titanium by sulfur. The lower energy titanium peak values at around 457 eV and 460 eV confirms the contribution of Ti^{3+} [47,48], and suggests the formation of Ti-O-S bonds [26,49].

Fig. 4a-d shows the O 1s XPS spectra of undoped and sulfur-doped TiO_2 films. The peaks located at 530.5 eV for TiO_2, 529.6 eV for 0.2 at.% S, 529.9 eV for 3 at.% S, and 529.3 eV for 8 at.% S into TiO_2 correspond to oxygen in TiO_2 lattice (Ti-O-Ti) [3,44,45]. Sulfur-doped TiO_2 films exhibited a small peak centered at around 531 eV, which can be attributed to the O_2/OH^- adsorbed on the TiO_2 surface [35,36, 49]. From the heat treatment, the H_2O molecules adsorbed on the film surface dissociate into OH^- hydroxyl groups and H^+ ions [24,50,51]. However, temperature increase results in a reduction of water molecules adsorbed in the surface. The displacement of Ti 2p and O 1s peaks for sulfur-doped films is similar. Anitha et al. [35] suggest that this displacement may promote the formation of intermediate energy levels between the conduction band (CB) and the valence band (VB) of TiO_2 films due to sulfur presence. The high-resolution XPS spectra of Ti 2p and O 1s peaks suggest the formation of oxygen vacancies on the sulfur-doped surface or even in the bulk, which can reduce the bandgap into the films and limit the electron (e^-)/hole (h^+) recombination [49].

3.2. Structural characterization

The functional groups formed on the undoped and sulfur doped films surface can be identified in the FTIR spectra shown in Fig. 5. The films exhibited similar profile spectra with an absorption band in the range 500-700 cm^{-1}, attributed to the symmetrical stretching vibration of Ti—O bonds [14,36,45]. The absorption band at 1630 cm^{-1} may be related to the OH^- of water molecules adsorbed on the films surface [24, 49], also found in the XPS analyses. Compared to the undoped TiO_2 film, the sulfur-doped films spectra presented two additional absorbance peaks around 1040 cm^{-1} and 1135 cm^{-1}, which suggest the presence of Ti—O—S bonds [37] and confirms the incorporation of sulfur atoms into the TiO_2 structure [35].

The peak centered at 1135 cm^{-1} found in all the doped films, represents a S—O vibration characteristic of the SO_4^{2-} functional group coordinated to the Ti^{4+} ion [52]. Several studies have demonstrated that the substitution of Ti^{4+} ions by S^{6+} cations, forming a Ti—O—S bond into the sulfur-doped TiO_2 crystal structure, may result in the formation of two possible coordination models, as proposed in Fig. 6.

The major steps in the sulfur doping mechanism of the TiO_2 by the H_2S decomposition may be summarized by Eqs. (1)-(7). When anatase-TiO_2 (in bulk) is energetically activated, either from heat treatment or light irradiation, it absorbs the energy of the process (E_g for anatase-TiO_2: 3.26 eV), and excites the electrons from VB to CB. In this electronic transition, electron (e^-)/hole (h^+) pairs are generated, forming

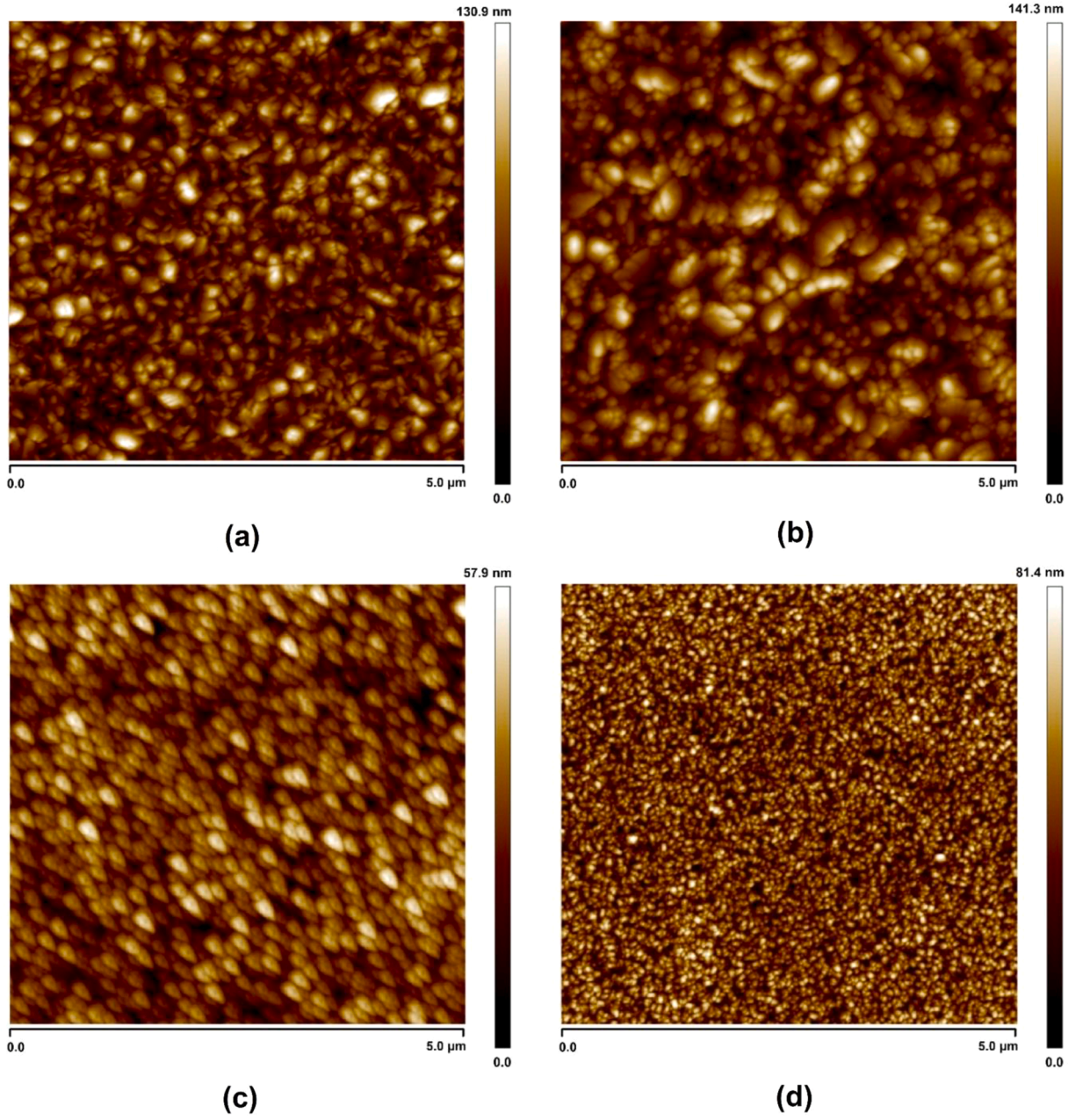

Fig. 8. AFM topography images of TiO_2 films grown at 400 °C on borosilicate glass substrate: (a) undoped TiO_2 film; (b) 0.2 at.% S into TiO_2 film; (c) 3 at.% S into TiO_2 film; (d) 8 at.% S into TiO_2 film.

Table 2
Sulfur-doping effect on the morphology characteristics of TiO_2 films grown at 400 °C on borosilicate glass substrates.

	Film thickness (nm)	Mean grain size (nm)	RMS roughness (nm)	Mean contact angle measurements
Undoped TiO_2	468	217	16.4	62°
0.2 at.% S-TiO_2	471	221	16.2	55°
3 at.% S-TiO_2	473	178	12.7	16°
8 at.% S-TiO_2	465	104	8.6	12°

oxidizing and reducing sites on the film surface. The water molecules present in the system will first dissociate to H^+ and OH^- ions. Hydroxyl oxidant species are produced when the OH^- ions donate one electron (e^-) to the hole (h^+), which allows the H_2S molecules oxidation [50]. The H_2S adsorbed reacts with the $^{\bullet}OH$ formed, and oxidizes into the form of SO_4^{2-} groups [24,26,51], promoting the surface modification and sulfur doping of the TiO_2. Alternatively, the H_2O_2 formed from the H_2O and O_2 reaction can oxidize the adsorbed H_2S. The events occur in the order described, without any need of using oxidizing agents or stabilizing compounds.

$$TiO_2\ e^- + h^+ \quad (1)$$

$$h^+ + H_2O_{ads} \rightarrow {}^{\bullet}OH + H^+ \quad (2)$$

$$h^+ + OH^-{}_{superf} \rightarrow {}^{\bullet}OH \quad (3)$$

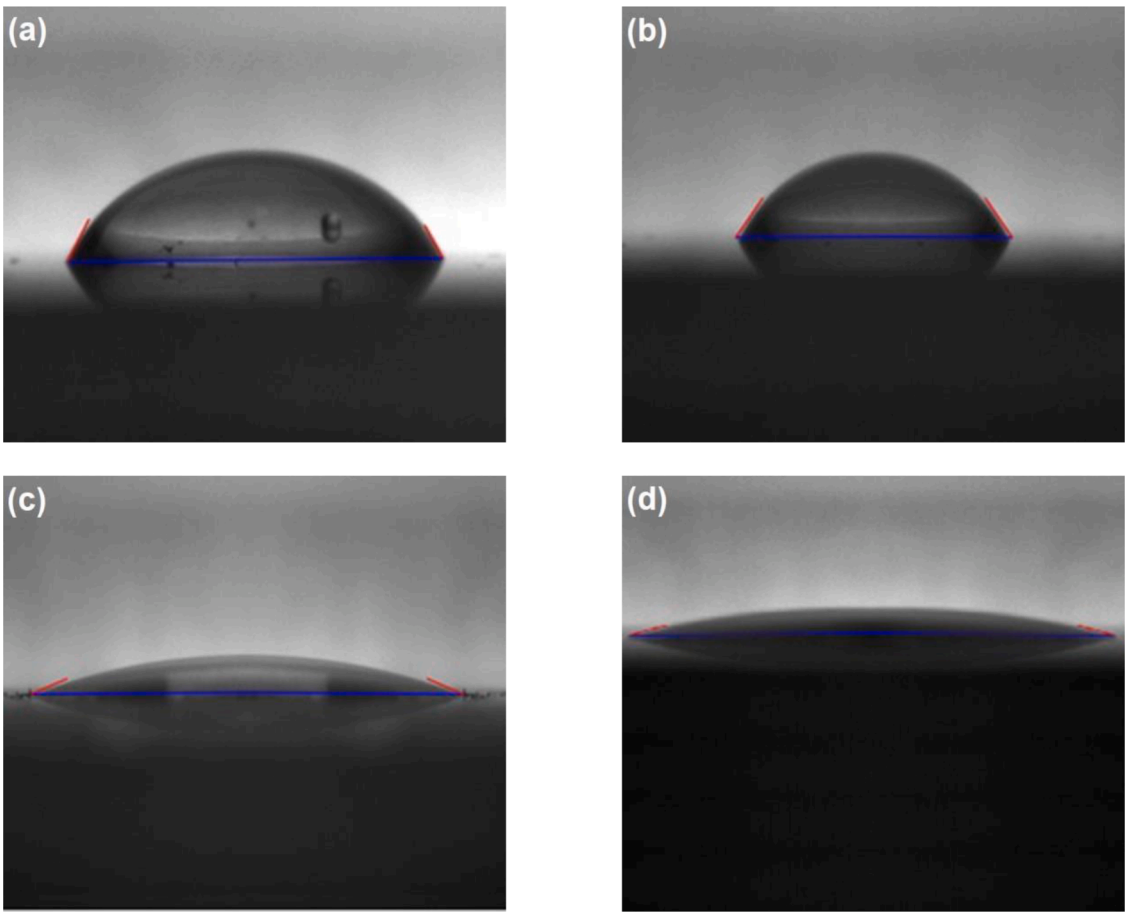

Fig. 9. Deionized water drop profile (5 μL) on the surface of films grown at 400 °C on borosilicate glass: (a) undoped TiO_2 film; (b), 0.2 at.% S into TiO_2 film; (c) 3 at.% S into TiO_2 film; (d) 8 at.% S into TiO_2 film.

$$2e^- + O_2 + 2H_2O \rightarrow H_2O_2 \quad (4)$$

$$H_2S_{gas} \rightarrow H_2S_{ads} \quad (5)$$

$$H_2S_{ads} + 8^{\bullet}OH \rightarrow SO_4^{2-} + 2H^+ + 4H_2O \quad (6)$$

$$H_2S_{ads} + 4H_2O_2 \rightarrow SO_4^{2-} + 2H^+ + 4H_2O \quad (7)$$

The TiO_2 films exhibit crystalline character associated with peaks corresponding to 2θ angles of 25.3°, 47.9°, 55.1°, 70.3° and 76.2°, respectively related to the anatase (JCPDS 211272) crystallographic planes (101), (200), (211), (220), and (301) [26,53] as it can be seen in Fig. 7. The crystalline phase did not alter after the sulfur-doping process and it is in agreement with results shown in the literature [15,35].

3.3. Morphological characterization

Fig. 8a-d presents the AFM topography images of the undoped and sulfur-doped TiO_2. The films are composed of round well-defined grains, without the presence of cracks or pores, and presents grains uniformly distributed on the substrate surface. The RMS roughness of the films varied between 8-16 nm as it can be seen in Table 2. It is observed that the TiO_2 films containing 3 at.% S and 8 at.% S presented a reduction of the RMS roughness values and grain size refinement, compared to the same parameters of the undoped TiO_2. Such behavior can be due to the formation of SO_4^{2-} groups on the TiO_2 surface during the H_2S decomposition and adsorption process under H_2 reducing atmosphere [25,26,45]. The 0.2 at.% S into TiO_2 film did not demonstrate significant morphological changes.

Surface wettability is associated to the tendency of a liquid to spread on the surface. Fig. 9a-d show the drop profile obtained in the goniometer, as well as the contact angle measurements formed between the drop and the films surface. It is observed that the water droplet contact angle increases with the sulfur concentration in TiO_2 films, presenting mean values ranging from 12° to 62°, as shown in Table 2. The results confirm a higher hydrophilicity of the sulfur-doped films, particularly the 8 at% S into TiO_2 (Fig. 9d). Xiong et al. [54] and Nishikiori et al. [55] reported that roughness is one of the main parameters that can alter the wettability behavior of a film. Reduction of the roughness values provides an increase in the surface free energy and, consequently, its affinity by the H_2O molecules.

3.4. Cross-section of the films

Fig. 10a-d show the FE-SEM cross-sectional images of undoped and sulfur-doped TiO_2 films grown at 400 °C on borosilicate substrates by MOCVD process. It can be observed that the interface between the film and the substrate is flat and adherent. The films grow perpendicular to the surface of the substrate. The FE-SEM images reveal the formation of a dense film that shows columnar morphology, characteristic structure of TiO_2 films grown by MOCVD [14,26,56]. In our previous studies it was pointed out the existence of an ideal thickness – around 470 nm – in which the catalyst presents better dye removal behavior [27]. Thinner films present a higher photogenerated charges recombination rate, due to the difficulty in transferring the electron (e^-)/ hole (h^+) pairs [27,57]. However, the increase in thickness difficults the electronic mobility, as it causes the photons to travel greater distances given the light penetration depth required to activate the semiconductor and produce the hydroxyl radicals [58]. By evaluating the FE-SEM images, the film thickness values were estimated, and presented in Table 2. The results indicated that the films preserved the same thickness after the sulfur

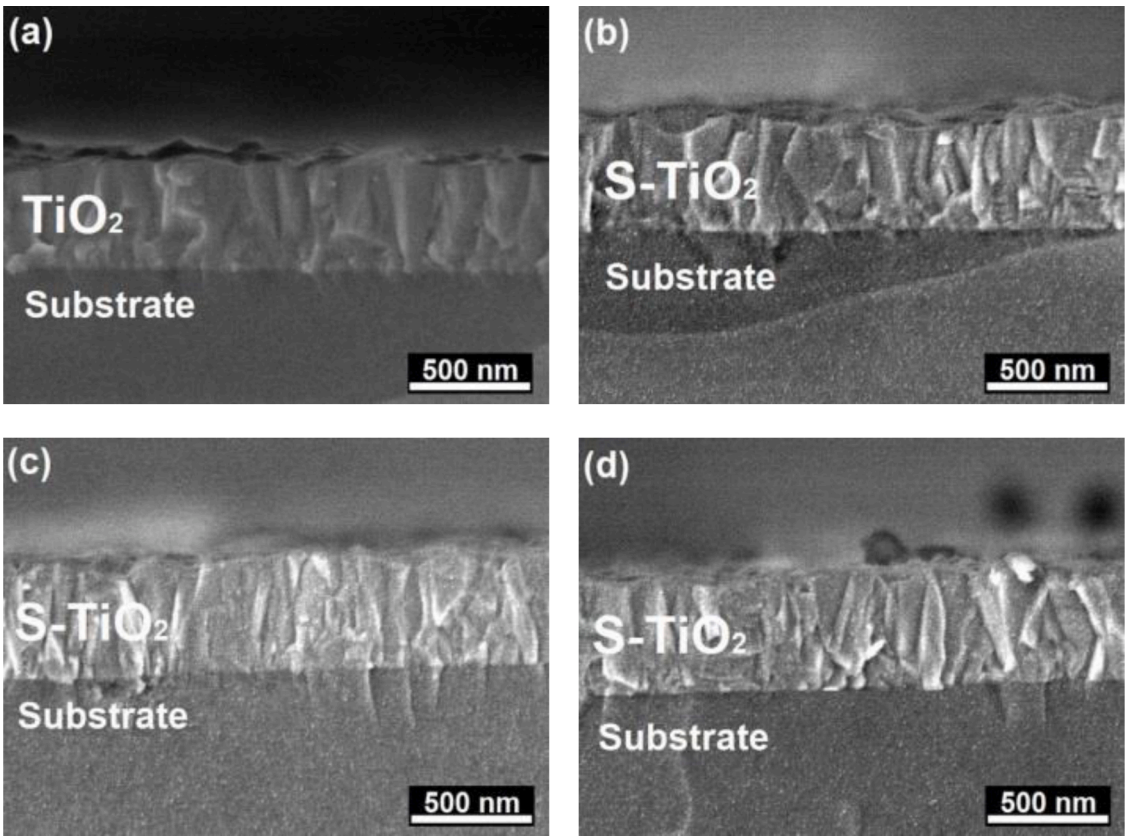

Fig. 10. Cross-sectional FE-SEM images of TiO_2films grown at 400 °C on borosilicate glass substrates by MOCVD: (a) undoped TiO_2 film, (b) 0.2 at.% S into TiO_2 film, (c) 3 at.% S into TiO_2 film, and (d) 8 at.% S into TiO_2 film.

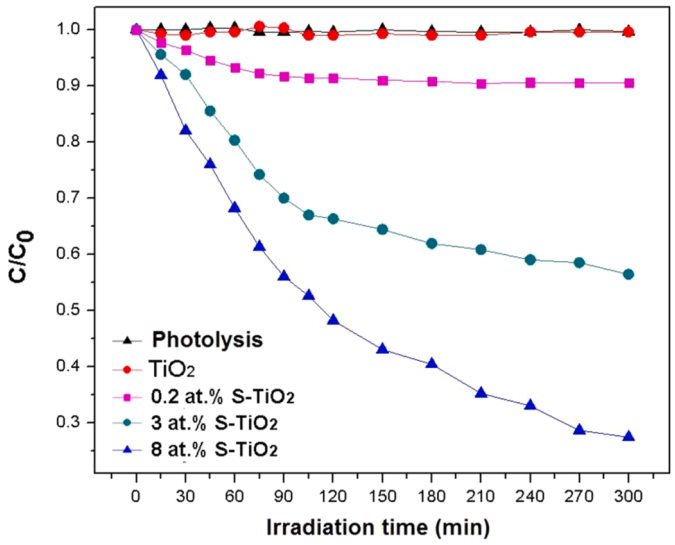

Fig. 11. Photocatalytic behavior of undoped and sulfur-doped TiO_2 films grown at 400 °C on the methyl orange dye decolorization under visible light irradiation for 300 min.

doping process. The growth rate of the films is linear, and it was estimated by dividing the film thickness by the growth time. The value found was of 12 nm.min^{-1} for all the films grown at 400 °C.

3.5. Photocatalytic behavior of the films

Surface modification of the TiO_2 films promotes its photoactivation in the visible light region of the electromagnetic spectrum, and presents a promising step, due to the possibility of optimizing the use of solar radiation. The sulfur-doping at low temperatures, resulting from H_2S decomposition is an alternative doping route and induced morphological modifications on the films surface. The surface modification effects on the films photocatalytic properties were evaluated on the methyl orange dye decolorization (Fig. 11). The photolysis curve demonstrates that no decolorization is observed without the film. The 8 at.% S into TiO_2 film exhibited the best photocatalytic activity, with a performance of 72.1 %. Undoped anatase-TiO_2 film did not present photocatalytic activity under visible light. Other studies showed the same trend [26,55,59]. The 0.2 at.% and 3 at.% S into TiO_2 films showed 9.6 % and 44.3 %, respectively. The results suggest the surface influence of grain size and roughness on the photocatalytic efficiency of the films [9,14,27]. The SO_4^{2-} groups on the surface of the TiO_2 increase its specific surface area [35,60]. In this condition, the contact between the catalyst and the dye, and also with the light is enhanced which increase the photocatalytic efficiency [34]. The surface roughness of the films influences its photocatalytic behavior and the determined RMS values are considered appropriated for photocatalytic applications, since it favors the contact between the adsorbed substances and the film, enhancing its photocatalytic efficiency [3,61]. Lower roughness values enable a homogeneous distribution of grain sizes on the films surface [62], which also contributes to increase the specific surface area and improves their photocatalytic activity. Studies by Kim et al. [63] indicate that the photocatalytic activity of TiO_2 films decreases as the surface roughness increases, similar to the results obtained in the present paper. Hot et al. [64] suggest that, although roughness increase favors the contact between the catalyst and the pollutant, it does not necessarily boost its photocatalytic character. The authors propose the existence of an ideal roughness value for which films achieve the best photocatalytic performance.

The doped TiO_2 films obtained here show practical and efficient use under visible light. It was possible to observe that the photocatalytic behavior of the sulfur-doped films is dependent on the S content in the structure. The SO_4^{2-} groups on the sulfur-doped catalysts stimulated the formation of a highly photoactivated surface [26,38]. The cationic substitution of the Ti^{4+} by S^{6+} ions results in the formation of Ti—O—S bonds, which changes the electronic sites from O 2p atomic orbital to S 3p atomic orbital [35,65]. The oxygen atom becomes a deficient center that hinders the recombination rate of the electron (e^-)/hole (h^+) pairs under visible light [15,36], and increases the formation of $^{\bullet}OH$ radicals. Also, such a hydrophilic character helps to keep the water molecules closer to the film surface, and it facilitates the efficiency of electrons transfer. The OH^- groups of the water molecules adsorbed on the hydrophilic surface favor the formation of the $^{\bullet}OH$ active species, which increases the photocatalytic activity of the film.

The photocatalytic behavior of the sulfur-doped TiO_2 films under visible light can be described by Eqs. (8)-(17). During the photocatalytic process, the sulfate species are oxidized by O_2 and promote the electrons (e^-) transition to the catalyst surface, producing the superoxide radical $O_2^{-\bullet}$, as shown in Eq. 13 [15,65]. The holes (h^+) formed react with the OH^- hydroxyl anion adsorbed on the sulfur-doped TiO_2 surface to produce $^{\bullet}OH$, according to Eqs. (14) and (15) [36], which promotes the oxidation of organic molecules and ionized species (Eq. (16)). All occurrences mentioned require water and dissolved oxygen to occur. In the absence of water, it would not be possible to form the $^{\bullet}OH$ radicals.

$$(SO_4^{2-} - TiO_2) + h\nu \rightarrow e^-_{cb} + h^+_{vb} \quad (8)$$

$$e^-_{cb} + 2H^+_{ads} \rightarrow H_2 \quad (9)$$

$$e^-_{cb} + H_2O_{ads} \rightarrow H^+ + OH^- \quad (10)$$

$$Ti^{4+} + e^-_{cb} \rightarrow Ti^{3+} \quad (11)$$

$$S^{6+} + Ti^{3+} \rightarrow S^{5+} + Ti^{4+} \quad (12)$$

$$S^{5+} + O_2 \rightarrow S^{6+} + O_2^{\bullet-} \quad (13)$$

$$h^+_{vb} + H_2O_{ads} \rightarrow H^+ + {}^{\bullet}OH \quad (14)$$

$$S^{5+} + h^+_{vb} + OH^-_{ads} \rightarrow S^{4+} + {}^{\bullet}OH \quad (15)$$

$$Dye + O_2^{\bullet-} + {}^{\bullet}OH \rightarrow degradation\ products \quad (16)$$

$$e^-_{cb} + h^+_{vb} \rightarrow Heat \quad (17)$$

The results showed that the TiO_2 films grown by MOCVD, and subsequently sulfur-doped at low temperatures by the H_2S decomposition may be promising catalysts for environmental applications with high efficiency. The study allows observing that the SO_4^{2-} groups present on the surface of the films as a result of the introduction of sulfur by the doping process form a nanostructure favorable to the capture of the photogenerated charges. These charges, consequently, reduce the electron (e^-)/hole (h^+) pairs recombination rate and promote the efficient formation of highly degraded transient species [15]. Thus, the photocatalytic behavior of the TiO_2 films is improved, enabling their practical use under sunlight irradiation or indoors using visible light bulbs.

4. Conclusions

In this study sulfur-doped TiO_2 films were produced by an alternative route at low temperature. It was observed that the sulfur content present in the films decreased as the doping temperature increased in the range 50° – 150 °C. The sulfur-doping process did not alter the crystalline structure of the films that remains anatase in all the situations. Ti—O—S bonds were formed into the TiO_2 lattice indicating the substitution of Ti^{4+} ions by S^{6+} whereas SO_4^{2-} groups were formed on the films surface. Sulfur-doping mechanism of TiO_2 films under H_2/H_2S atmosphere was proposed. The increase in the S content in the films promoted morphological modifications and increased the hydrophilicity of the films which, consequently, provides the increase of its photocatalytic activity. The photocatalytic experiments demonstrated that the sulfur-doped films can be efficient on the methyl orange dye decolorization under visible light irradiation, while the undoped film did not show photoactivity. The 8 at.% S-doped TiO_2 film exhibited the best photocatalytic activity showing 72.1 % of dye decolorization after 300 min of exposition. These results suggest that visible light activated sulfur-doped TiO_2 films can be considered for use in environmental applications in water treatment.

Declaration of Competing Interest

The authors declare that they have no known competing financial interests or personal relationships that could have appeared to influence the work reported in this paper.

Acknowledgments

The authors are grateful to the Brazilian agencies CAPES, CNPq (Proc. 168935/2018-0), and FAPESP (Proc. 05/55861-4) for the financial support. This research used resources of the Brazilian Nanotechnology National Laboratory (LNNano). The Nanostructured Materials Laboratory staff is acknowledged for kindly make available the XPS equipment and for the assistance during the experiments.

References

[1] A. Fujishima, K. Honda, Electrochemical photolysis of water at a semiconductor electrode, Nature 238 (1972) 37–38, https://doi.org/10.1038/238037a0.
[2] S. Cravanzola, F. Cesano, F. Gaziano, D. Scarano, Sulfur-doped TiO_2: structure and surface properties, Catalysts 7 (7) (2017) 214, https://doi.org/10.3390/catal7070214, 11 pp.
[3] R.T. Bento, M.F. Pillis, Titanium Dioxide Films for Photocatalytic Degradation of Methyl Orange Dye, in: Titanium Dioxide - Material for a Sustainable Environment. 1ed, InTech, London, 2018, pp. 211–226, https://doi.org/10.5772/intechopen.75528.
[4] Y.K. Abdel-Maksoud, E. Imam, A.R. Ramadan, Sand supported TiO_2 photocatalyst in a tray photo-reactor for the removal of emerging contaminants in wastewater, Catal. Today 313 (2018) 55–62, https://doi.org/10.1016/j.cattod.2017.10.029.
[5] M. Ge, C. Cao, J. Huang, S. Li, Z. Chen, K.-Q. Zhang, S.S. Al-Deyab, Y. Lai, A review of one-dimensional TiO_2 nanostructured materials for environmental and energy applications, J. Mater. Chem. A 4 (2016) 6772–6801, https://doi.org/10.1039/C5TA09323F.
[6] M. Ge, Q. Li, C. Cao, J. Huang, S. Li, S. Zhang, Z. Chen, K. Zhang, S.S. Al-Deyab, Y. Lai, One-dimensional TiO_2 nanotube photocatalysts for solar water splitting, Advanc. Sci. 4 (1) (2017), 1600152, https://doi.org/10.1002/advs.201600152.
[7] J. Cai, J. Shen, X. Zhang, Y.H. Ng, J. Huang, W. Guo, C. Lin, Y. Lai, Light-driven sustainable hydrogen production utilizing TiO_2 nanostructures: a review, Small Methods 3 (1) (2019), 1800184, https://doi.org/10.1002/smtd.201800184.
[8] Q. Wang, J. Cai, G.V. Biesold-McGee, J. Huang, Y.N. Ng, H. Sun, J. Wang, Y. Lai, Z. Lin, Silk fibroin-derived nitrogen-doped carbon quantum dots anchored on TiO_2 nanotube arrays for heterogeneous photocatalytic degradation and water splitting, Nano Energy 78 (2020), 105313, https://doi.org/10.1016/j.nanoen.2020.105313.
[9] H.O. Pierson, Handbook of chemical vapor deposition (CVD) – Principles, technology and applications, Noyes Publications, 1999, 2ª ed.
[10] K.M. Reza, A.S.W. Kurny, F. Gulshan, Parameters affecting the photocatalytic degradation of dyes using TiO_2: a review, Appl. Water Sci. 7 (2017) 1569–1578, https://doi.org/10.1007/s13201-015-0367-y.
[11] R. Guz, C. Moura, M.A.A. Cunha, Factorial design application in photocatalytic wastewater degradation from TNT industry-red water, Environ. Sci. Pollut. Res. Int. 24 (2017) 6055–6060, https://doi.org/10.1007/s11356-016-6460-4.
[12] A.T. Montoya, E.G. Gillan, Enhanced photocatalytic hydrogen evolution from transition-metal surface-modified TiO_2, ACS Omega 3 (2018) 2947–2955, https://doi.org/10.1021/acsomega.7b02021.
[13] A. Piatkowska, M. Janus, K. Szymanski, S. Mozia, C-,N- and S-doped TiO_2 photocatalysts: a review, Catalysts 11 (2021) 144, https://doi.org/10.3390/catal11010144.
[14] E.C. de Oliveira, R.T. Bento, O.V. Correa, M.F. Pillis, Visible-light photocatalytic activity and recyclability of N-doped TiO_2 films grown by MOCVD, Cerâmica 66 (380) (2020) 451–459, https://doi.org/10.1590/0366-69132020663802957.
[15] F. Zhang, M. Wang, X. Zhu, B. Hong, W. Wang, Z. Qi, W. Xie, J. Ding, J. Bao, S. Sun, C. Gao, Effect of surface modification with H_2S and NH_3 on TiO_2 for adsorption and photocatalytic degradation of gaseous toluene, Appl. Catal. B. Environ. 170-171 (2015) 215–224, https://doi.org/10.1016/j.apcatb.2015.01.045.
[16] D. Li, H. Haneda, S. Hishita, N. Ohashi, N.K. Labhsetwar, Fluorine-doped TiO_2 powders prepared by spray pyrolysis and their improved photocatalytic activity for decomposition of gas-phase acetaldehyde, J. Fluorine Chem. 126 (2005) 69–77, https://doi.org/10.1016/j.jfluchem.2004.10.044.

[17] A. McGuiness, J. Baltrusaitis, R. Nessler, Synthesis and characterization of chlorine and bromine doped TiO_2 nanoparticles for photocatalytic methanol production, Microsc. Microanal. 17 (2011) 1704–1705, https://doi.org/10.1017/S1431927611009391.

[18] S. Kataoka, E. Lee, M.I. Tejedor-Tejedor, M.A. Anderson, Photocatalytic degradation of hydrogen sulfide and in situ FT-IR analysis of reaction products on surface of TiO_2, Appl. Catal. B. Environ. 61 (2005) 159–163, https://doi.org/10.1016/j.apcatb.2005.04.018.

[19] C. Liu, R. Zhang, S. Wei, J. Wang, Y. Liu, M. Li, R. Liu, Selective removal of H_2S from biogas using a regenerable hybrid TiO_2/zeolite composite, Fuel 157 (2015) 183–190, https://doi.org/10.1016/j.fuel.2015.05.003.

[20] G. Liu, J. Ji, P. Hu, S. Lin, H. Huang, Efficient degradation of H_2S over transition metal modified TiO_2 under VUV irradiation: Performance and mechanism, App. Surf. Sci. 433 (2018) 329–335, https://doi.org/10.1016/j.apsusc.2017.09.257.

[21] X. Hao, G. Hou, P. Zheng, R. Liu, C. Liu, H_2S in-situ removal from biogas using a tubular zeolite/TiO_2 photocatalytic reactor and the improvement on methane production, Chem. Eng. J. 294 (2016) 105–110, https://doi.org/10.1016/j.cej.2016.02.098.

[22] A. Alonso-Tellez, D. Robert, N. Keller, V. Keller, A parametric study of the UV-A photocatalytic oxidation of H_2S over TiO_2, Appl. Catal. B. Environ. 115–116 (2012) 209–218, https://doi.org/10.1016/j.apcatb.2011.12.014.

[23] R. Portela, B. Sanchéz, J.M. Coronado, Photocatalytic oxidation of H_2S on TiO_2 and TiO_2-ZrO_2 thin films, J. Adv. Oxid. Technol. 10 (2) (2007) 375–380, https://doi.org/10.1515/jaots-2007-0223.

[24] M.C. Canela, R.M. Alberici, W.F. Jardim, Gas-phase destruction of H_2S using TiO_2/UV-VIS, J. Photochem. Photobiol. A 112 (1998) 73–80, https://doi.org/10.1016/S1010-6030(97)00261-X.

[25] Y. Chen, Y. Jiang, W. Li, R. Jin, S. Tang, W. Hu, Adsorption and interaction of H_2S/SO_2 on TiO_2, Catal. Today 50 (1999) 39–47, https://doi.org/10.1016/S0920-5861(98)00460-X.

[26] R.T. Bento, O.V. Correa, M.F. Pillis, Photocatalytic activity of undoped and sulfur-doped TiO_2 films grown by MOCVD for water treatment under visible light, J. Europ. Ceram. Soc. 39 (2019) 3498–3504, https://doi.org/10.1016/j.jeurceramsoc.2019.02.046.

[27] B.A. Marcello, O.V. Correa, R.T. Bento, M.F. Pillis, Effect of growth parameters on the photocatalytic performance of TiO_2 films prepared by MOCVD, J. Braz. Chem. Soc. 31 (2020) 1270–1283. http://doi.org/10.21577/0103-5053.20200012.

[28] J. Walton, P. Wincott, N. Fairley, A. Carrick, Peak Fitting with CasaXPS. A Casa Pocket Book, 2010.

[29] X. Li, D. Wang, G. Cheng, Q. Luo, J. An, Y. Wang, Preparation of polyaniline-modified TiO_2 nanoparticles and their photocatalytic activity under visible light illumination, Appl. Catal. B. Environ. 81 (2008) 267–273, https://doi.org/10.1016/j.apcatb.2007.12.022.

[30] C. Shao, G. Zhou, Z. Li, Y. Wu, D. Xu, B. Sun, Fabrication of large diameter tube-like mesoporous TiO_2 via homogeneous precipitation and photocatalytic decomposition of papermaking wastewater, Chem. Eng. J. 230 (2013) 227–235, https://doi.org/10.1016/j.cej.2013.06.084.

[31] A. Ahmadpour, M. Zare, M. Behjoomanesh, M. Avazpour, Photocatalytic decolorization of methyl orange dye using nano-photocatalysts, Adv. Environ. Technol 3 (2015) 121–127. http://doi.org/10.22104/aet.2015.371.

[32] L. Pan, J.-J. Zou, S. Wang, Z.-F. Huang, X. Zhang, L. Wang, Enhancement of visible-light-induced photodegradation over hierarchical porous TiO_2 by nonmetal doping and water-mediated dye sensitization, Appl. Surf. Sci. 268 (2013) 252–258, https://doi.org/10.1016/j.apsusc.2012.12.074.

[33] D. Duc La, A. Rananaware, H.P. NguyenThi, L. Jones, S.V. Bhosale, Fabrication of a TiO_2@porphyrin nanofiber hybrid material: a highly efficient photocatalyst under simulated sunlight irradiation, Adv. Nat. Sci. Nanosci. Nanotechnol. 8 (2017), 015009, https://doi.org/10.1088/2043-6254/aa597e.

[34] F. Wang, F. Li, L. Zhang, H. Zeng, Y. Sun, S. Zhang, X. Xu, S-TiO_2 with enhanced visible-light photocatalytic activity derived from TiS_2 in deionized water, Mat. Res. Bul. 87 (2017) 20–26, https://doi.org/10.1016/j.materresbull.2016.11.014.

[35] B. Anitha, C. Ravidhas, R. Venkatesh, A.M.E. Raj, K. Ravichandran, B. Subramanian, C. Sanjeeviraja, Self assembled sulfur induced interconnected nanostructure TiO_2 electrode for visible light photoresponse and photocatalytic application, Physica E. Low Dimens. Syst. Nanostruct. 91 (2017) 148–160, https://doi.org/10.1016/j.physe.2017.04.017.

[36] L.G. Devi, R. Kavitha, Enhanced photocatalytic activity of sulfur doped TiO_2 for the decomposition of phenol: A new insight into the bulk and surface modification, Mat. Chem. Phys. 143 (2014) 1300–1309, https://doi.org/10.1016/j.matchemphys.2013.11.038.

[37] C. Han, M. Pelaez, V. Likodimos, A.G. Kontos, P. Falaras, K. O'Shea, D. D. Dionysiou, Innovative visible light-activated sulfur doped TiO_2 films for water treatment, Appl. Catal. B Environ. 107 (2011) 77–87, https://doi.org/10.1016/j.apcatb.2011.06.039.

[38] T. Ohno, M. Akiyoshi, T. Umebayashi, K. Asai, T. Mitsui, M. Matsumura, Preparation of S-doped TiO_2 photocatalysts and their photocatalytic activities under visible light, Appl. Catal. A. Gen. 265 (2004) 115–121, https://doi.org/10.1016/j.apcata.2004.01.007.

[39] Q. Sun, J. Zhanga, P. Wang, J. Zheng, X. Zhang, Y. Cui, J. Feng, Y. Zhu, Sulfur-doped TiO_2 nanocrystalline photoanodes for dye-sensitized solar cells, J. Renew. Sustain. Energy 4 (2012), 023104, https://doi.org/10.1063/1.3694121.

[40] Y.-H. Lin, S.-H. Chou, H. Chu, A kinetic study for the degradation of 1,2-dichloroethane by S-doped TiO_2 under visible light, J. Nanopart. Res. 16 (8) (2014) 1–12, https://doi.org/10.1007/s11051-014-2539-3.

[41] F. Zhang, M. Wang, X. Zhu, B. Hong, W. Wang, Z. Qi, W. Xie, J. Ding, J. Bao, S. Sun, C. Gao, Effect of surface modification with H_2S and NH_3 on TiO_2 for adsorption and photocatalytic degradation of gaseous toluene, Appl. Catal. B. Environ. 170-171 (2015) 215–224, https://doi.org/10.1016/j.apcatb.2015.01.045.

[42] T. Ohno, N. Murakami, Development of visible-light active S cation-doped TiO_2 photocatalyst, Curr. Org. Chem. 14 (7) (2010) 699–708, https://doi.org/10.2174/138527210790963386.

[43] T. Umebayashi, T. Yamaki, H. Itoh, K. Asai, Band gap narrowing of titanium dioxide by sulfur doping, Appl. Phys. Lett. 81 (3) (2002) 454–456, https://doi.org/10.1063/1.1493647.

[44] R. Liu, X. Zhou, F. Yang, Y. Yu, Combination study of DFT calculation and experimente for photocatalytic properties of S-doped anatase TiO_2, Appl. Surf. Sci. 319 (2014) 50–59, https://doi.org/10.1016/j.apsusc.2014.07.132.

[45] G. Yang, Z. Yan, T. Xiao, Low-temperature solvothermal synthesis of visible-light-resposive S-doped TiO_2 nanocrystal, Appl. Surf. Sci. 258 (8) (2012) 4016–4022, https://doi.org/10.1016/j.apsusc.2011.12.092.

[46] S.A. Bakar, C. Ribeiro, A comparative run for visible-light-driven photocatalytic activity of anionic and cationic S-doped TiO_2 photocatalysts: a case study of possible sulfur doping through chemical protocol, J. Mol. Catal. A Chem. 421 (2016) 1–15, https://doi.org/10.1016/j.molcata.2016.05.003.

[47] P. Georgios, S.M. Wolfgang, X-ray photoelectron spectroscopy of anatase-TiO_2 coated carbon nanotubes, Solid State Phenom. 162 (2010) 163–177, https://doi.org/10.4028/www.scientific.net/SSP.162.163.

[48] M. Dhayal, R. Kapoor, P.G. Sistla, R.R. Pandey, S. Kar, K.K. Saini, G. Pande, Strategies to prepare TiO_2 thin films, doped with transition metal ions, that exhibit specific physicochemical properties to support osteoblast cell adhesion and proliferation, Mater. Sci. Eng. C Mater. Biol. Appl. 37 (2014) 99–107, https://doi.org/10.1016/j.msec.2013.12.035.

[49] M. Li, Z. Xing, J. Jiang, Z. Li, J. Kuang, J. Yin, N. Wan, Q. Zhu, W. Zhou, In-situ Ti^{3+}/S doped high thermostable anatase TiO_2 nanorods as efficient visible-light driven photocatalysts, Mater. Chem. Phys. 219 (2018) 303–310, https://doi.org/10.1016/j.matchemphys.2018.08.051.

[50] N. Shahzad, S.T. Hussain, A. Siddiqua, M.A. Baig, A comparison of TiO_2 nanoparticles and nanotubes for catalytic gas phase destruction of H_2S gas at high temperatures, J. Nanosci. Nanotechnol. 12 (6) (2012) 5061–5065, https://doi.org/10.1166/jnn.2012.4934.

[51] R.T. Bento, O.V. Correa, M.F. Pillis, On the surface chemistry and the reuse of sulfur-doped TiO_2 films as photocatalysts, Mater. Chem. Phys. 261 (2021), 124231, https://doi.org/10.1016/j.matchemphys.2021.124231.

[52] D.I. Sayago, P. Serrano, O. Böhme, A. Goldoni, G. Paolucci, E. Román, J.A. Martín-Gago, A photoemission study of the SO_2 adsorption on TiO_2 (110) surfaces, Surf. Sci. 482-485 (2001) 9–14, https://doi.org/10.1016/S0039-6028(00)00998-5.

[53] N. Shatotri, D. Sud, A greener approach to synthesize visible light responsive nanoporous S-doped TiO_2 with enhanced photocatalytic activity, New J. Chem. 39 (3) (2015) 2217–2223, https://doi.org/10.1039/C4NJ01422G.

[54] Y. Xiong, D. He, R. Jaber, P.J. Cameron, K.J. Edler, Sulfur-doped cubic mesostructured titania films for use as a solar photocatalyst, J. Phys. Chem. C 121 (18) (2017) 9929–9937, https://doi.org/10.1021/acs.jpcc.7b01615.

[55] H. Nishikiori, M. Hayashibe, T. Fujii, Visible light-photocatalytic activity of sulfate-doped titanium dioxide prepared by the sol-gel method, Catalysts 3 (2013) 363–377, https://doi.org/10.3390/catal3020363.

[56] A.J. Gardecka, C. Bishop, D. Lee, S. Corby, I.P. Parkin, A. Kafizas, S. Krumdieck, High efficiency water splitting photoanodes composed of nanostructured anatase-rutile TiO2 heterojunctions by pulsed-pressure MOCVD, Appl. Catal. B 224 (2018) 904–911, https://doi.org/10.1016/j.apcatb.2017.11.033.

[57] A.R. Malagutti, H.A.J.L. Mourão, J.R. Garbin, C. Ribeiro, Deposition of TiO_2 and Ag:TiO_2 thin films by the polymeric precursor method and their application in the photodegradation of textile dyes, Appl. Catal. B, Environ. 90 (2009) 205–212, https://doi.org/10.1016/j.apcatb.2009.03.014.

[58] S.-C. Jung, S.-J. Kim, N. Imaishi, Y.-I. Cho, Effect of TiO_2 thin film thickness and specific surface area by low-pressure metal–organic chemical vapor deposition on photocatalytic activities, Appl. Catal. B, Environ. 55 (4) (2005) 253–257, https://doi.org/10.1016/j.apcatb.2004.08.009.

[59] C.W. Dunnill, Z.A. Aiken, A. Kafizas, J. Pratten, M. Wilson, D.J. Morgan, I. P. Parkin, White light induced photocatalytic activity of sulfur-doped TiO_2 thin films and their potential for antibacterial application, J. Mater. Chem. 19 (2009) 8747–8754, https://doi.org/10.1039/b913793a.

[60] X.L. Peng, M.M. Yao, F. Li, X.H. Sun, Microstructures and photocatalytic properties of S doped nanocrystalline TiO_2 Films, Particul. Sci. Technol. 30 (2012) 81–91, https://doi.org/10.1080/02726351.2010.551711.

[61] O. Carp, C.L. Huisman, A. Reller, Photoinduced reactivity of titanium dioxide, Prog. Solid State Chem. 32 (2004) 33–177, https://doi.org/10.1016/j.progsolidstchem.2004.08.001.

[62] W. Ho, J.C. Yu, S. Lee, Low-temperature hydrothermal synthesis of S-doped TiO_2 with visible light photocatalytic activity, J. Solid State Chem. 179 (4) (2006) 1171–1176, https://doi.org/10.1016/j.jssc.2006.01.009.

[63] H.J. Kim, S.M. Yoo, S. Yu, W.I. Lee, Photocatalytic behavior of TiO_2 films: thickness and roughness dependence, Rapid Commun. Photosci. 2 (2013) 1–8, https://doi.org/10.5857/RCP.2013.2.1.001.

[64] J. Hot, J. Topalov, E. Ringot, A. Bertron, Investigation on parameters affecting the effectiveness of photocatalytic functional coatings to degrade NO:TiO amount on surface, illumination, and substrate roughness, Int. J. Photoenergy 2017 (2017) 14, https://doi.org/10.1155/2017/6241615, 6241615.

[65] Y.-H. Lin, H.-T. Hsueh, C.-W. Chang, H. Chu, The visible light-driven photodegradation of dimethyl sulfide on S-doped TiO_2: characterization, kinetics, and reaction pathways, Appl. Catal. B Environ. 199 (2016) 1–10, https://doi.org/10.1016/j.apcatb.2016.06.024.